Nanoscale amphiphilic macromolecules as lipoprotein inhibitors: the role of charge and architecture

Jinzhong Wang[1]
Nicole M Plourde[3]
Nicole Iverson[2]
Prabhas V Moghe[2,3]
Kathryn E Uhrich[1]

[1]Department of Chemistry and Chemical Biology; [2]Department of Biomedical Engineering; [3]Department of Chemical and Biochemical Engineering, Rutgers University, Piscataway, NJ, USA

Abstract: A series of novel amphiphilic macromolecules composed of alkyl chains as the hydrophobic block and poly(ethylene glycol) as the hydrophilic block were designed to inhibit highly oxidized low density lipoprotein (hoxLDL) uptake by synthesizing macromolecules with negatively charged moieties (ie, carboxylic acids) located in the two different blocks. The macromolecules have molecular weights around 5,500 g/mol, form micelles in aqueous solution with an average size of 20–35 nm, and display critical micelle concentration values as low as 10^{-7} M. Their charge densities and hydrodynamic size in physiological buffer solutions correlated with the hydrophobic/hydrophilic block location and quantity of the carboxylate groups. Generally, carboxylate groups located in the hydrophobic block destabilize micelle formation more than carboxylate groups in the hydrophilic block. Although all amphiphilic macromolecules inhibited unregulated uptake of hoxLDL by macrophages, inhibition efficiency was influenced by the quantity and location of the negatively charged-carboxylate on the macromolecules. Notably, negative charge is not the sole factor in reducing hoxLDL uptake. The combination of smaller size, micellar stability and charge density is critical for inhibiting hoxLDL uptake by macrophages.

Keywords: polymeric micelles, amphiphilic macromolecules, highly oxidized low-density lipoproteins, scavenger receptor inhibition

Introduction

Atherosclerosis is a process characterized by the buildup of low density lipoproteins (LDL) within the vascular intima and ensuing interactions between macrophages and their extracellular matrix molecules; it is the single leading cause of death in America (Williams and Tabas 1995; Olsson et al 2001; Camejo et al 2002; Thom et al 2006). Recent advances in nanotechnology for cardiovascular health are abundant and include the application of nanosensors to monitor nitro-oxidative species (oxidative stress) produced in the failing heart (Malinski 2005), microarrays or microchips for the study of cardiovascular disease (Carella et al 2003), electrospun nanofibers as tissue engineered vascular grafts (He, Ma, et al 2005; He, Yong, et al 2005; Ma et al 2005), and carbon nanotubes implanted for anticoagulant and antithrombotic properties (Endo et al 2005; Meng et al 2005). In contrast to the implantable devices described above, an avenue of particular interest in nanotechnology is the use of a "nano-blocker" to prevent highly oxidized LDL (hoxLDL) uptake via scavenger receptors. Native LDL uptake is mediated by feedback inhibition, whereas binding of hoxLDL to macrophage scavenger receptors leads to unregulated cholesterol accumulation and foam cell formation. Thus, controlling binding to hoxLDL is an important focus for new atherosclerotic treatments (Brown and Goldstein 1983; Steinberg 1997).

Previous work on LDL uptake has focused on synthetic compounds that target and bind scavenger receptors, such as SR-A and CD36 that appear to be of primary importance

Correspondence: Kathryn E Uhrich
Department of Chemistry and Chemical Biology, Rutgers University, Piscataway, NJ 08854, USA
Tel +1 732 445 0361
Fax +1 732 445 7036
Email keuhrich@rutgers.edu

in atherogenesis (Yoshiizumi et al 2004; Boullier et al 2005; Broz et al 2005; Guaderrama-Diaz et al 2005). For example, phosphocholine as a ligand for CD36 has been shown to inhibit the binding of hoxLDL in CD36-expressing cells (Boullier et al 2005). In addition, sulfatide derivatives for targeting SR-A have been shown to reduce acetylated LDL binding and uptake (Yoshiizumi et al 2004). Although previous efforts to develop scavenger receptor blockers are encouraging, increased efficiency may be reached through the use of an organized 3D presentation of the targeting groups or a multifunctional particle to simultaneously target several scavenger receptors (Chnari et al 2006). To create a multifunctional nano-blocker, one could exploit the fact that all scavenger receptors share an affinity for anionic ligands (Krieger et al 1993).

We previously reported a unique series of polymers, amphiphilic scorpion-like macromolecules (AScM) (Tian et al 2004), that self-organize into micelles and not only act as a drug delivery system but also decrease hoxLDL's uptake. Previous results show promise for AScMs as a hydrophobic drug carrier in terms of low CMC (critical micelle concentration), low cytotoxicity, high drug loading efficiency, and sustained release (Djordjevic et al 2005; Tao and Uhrich 2006). These macromolecules consist of three major components: poly(ethylene glycol) (PEG), mucic acid, and aliphatic acid chains, as seen in Figure 1 (Tian et al 2004). These building blocks were chosen because they are naturally occurring or biocompatible compounds, and each component is joined by potentially biodegradable ester bonds. PEG contributes to the hydrophilicity and is used to prevent the non-specific adsorption of proteins, mucic acid is a multi-hydroxylated saccharide providing reaction sites for further modification of the polymer, and aliphatic acid chains control the polymer hydrophobicity.

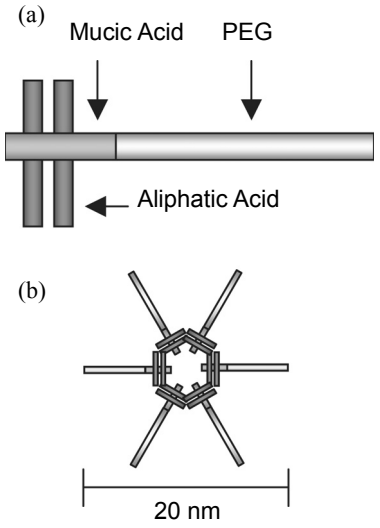

Figure 1 Schematic of an amphiphilic macromolecule: at concentrations greater than 10^{-7} M, the unimers in (a) self-aggregate to form micellar nanoparticles (b) with hydrodynamic diameters of ~20 nm.

Previous studies have focused on anionic AScMs that spontaneously form micelles at concentrations above the CMC (10^{-7}M) (Tian et al 2004). Each AScM is functionalized with a carboxylic acid, such that the micellar nanoparticle displays anionic charges in an organized and clustered configuration. The anionic AScMs reduced hoxLDL uptake by up to 80%, and both SR-A and CD36 receptors were involved in the uptake of the polymers and hoxLDL (Chnari et al 2005, 2006).

In this paper, we present a series of macromolecules that maintain two structural elements as previously described: mucic acid derivatives as the hydrophobic component and PEG as the hydrophilic component. For this investigation, the location and number of carboxylic acid groups were varied with our synthetic design; carboxylate groups can be precisely located in either the hydrophobic or hydrophilic domains, or in both domains (Figure 2).

The inhibition ability of these novel macromolecules for highly oxidized LDL by macrophages were studied as well as their solution properties, including micelle aggregation size, CMC and charge density.

Materials and methods

Chemical reagents for synthesis

Heterobifunctional poly(ethylene glycol) ($HCl{\cdot}NH_2$-PEG-COOH) with molecular weight of 5000 Da was obtained from Nektar (San Carlos, CA). 4-(Dimethylamino) pyridinium *p*-toluenesulfonate (DPTS) was prepared as previously described. Monomethoxy-poly(ethylene glycol) (mPEG) with molecular weights of 5000 Da was purchased from Sigma-Aldrich. All PEG reagents were dried by azeotropic distillation with toluene. β-Glutamic acid, 5-aminoisophthalic acid, 4-hydroxybenzoic acid, N-hydroxyl succinimide (NHS), triethylamine (99.7%) and 1,3-dicyclohexylcarbodiimide (DCC) in 1 M methylene chloride solution were purchased from Aldrich and used as received. All other reagents and solvents were reagent grade and used as received.

Macromolecules 1CM, 0CM and 1CP

The macromolecules **1CM**, **0CM** and **1CP** were prepared as previously described (Tian et al 2004; Chnari et al 2006).

Chemical characterization

Chemical structures and compositions were confirmed by ^1H and ^{13}C NMR spectroscopy with samples (~5–10 mg/ml)

dissolved in $CDCl_3$ solvent on Varian 400 MHz spectrometers, using tetramethylsilane as the reference signal. IR spectra were recorded on a Mattson Series spectrophotometer (Madison Instruments, Madison, WI) by solvent (methylene chloride) casting on a KBr pellet. Negative ion-mass spectra were recorded with a ThermoQuest Finnigan LCQ$^{TM}_{DUO}$ System (San Jose, CA) that includes a syringe pump, an optional divert/inject valve, an atmospheric pressure ionization (API) source, a mass spectrometer (MS) detector, and the Xcalibur data system. Meltemp (Cambridge, Mass) was used to determine the melting temperatures (T_m) of all the intermediates.

Gel permeation chromatography (GPC) was used to obtain molecular weight and polydispersity index (PDI). It was performed on Perkin-Elmer Series 200 LC system equipped with Pl gel column (5 μm, mixed bed, ID 7.8 mm, and length 300 mm) and with a Water 410 refractive index detector, Series 200 LC pump and ISS 200 Autosampler. Tetrahydrofuran (THF) was the eluent for analysis and solvent for sample preparation. Sample was dissolved into THF

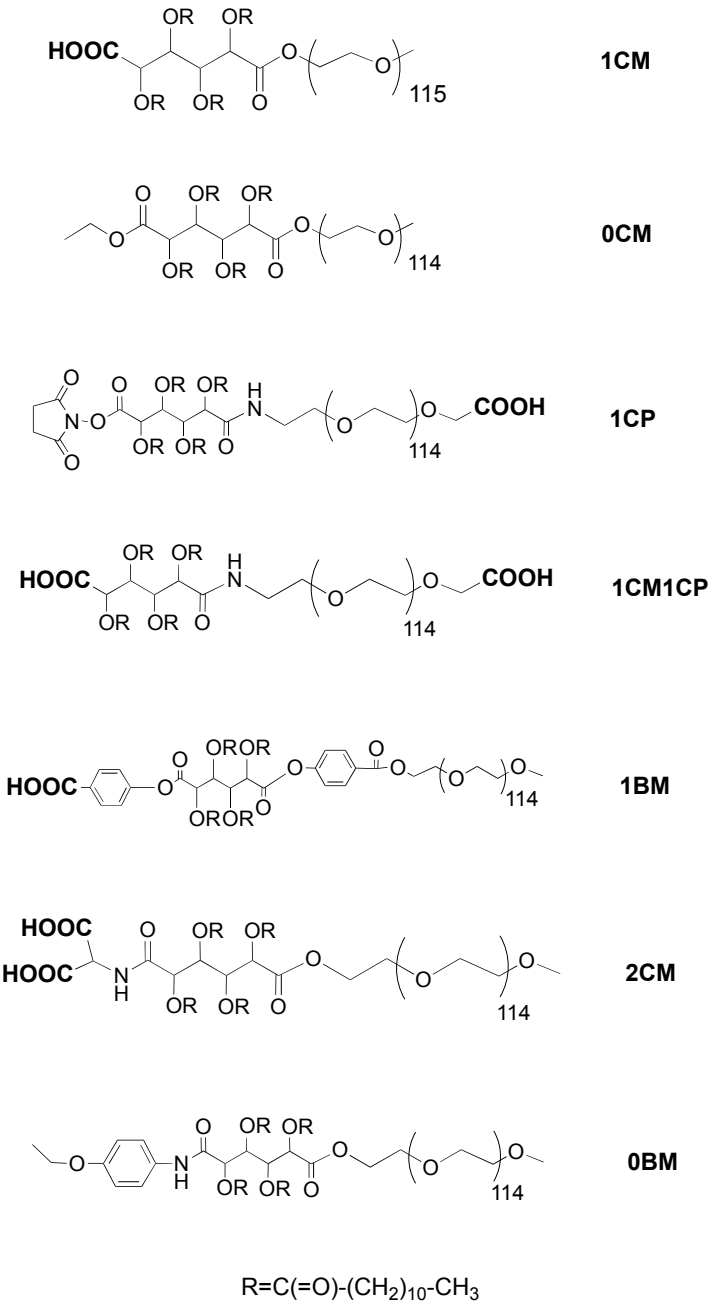

Figure 2 Nomenclature for amphiphilic macromolecules, where R in the chemical structures represents a lauroyl carbonyl group.

(~5 mg/ml) and filtered through a 0.45 μm PTFE syringe filter (Whatman, Clifton, NJ) before injection into the column at a flow rate of 1.0 ml/min. The average molecular weight of the sample was calibrated against narrow molecular weight polystyrene standards (Polysciences, Warrington, PA).

Synthesis of 1CM1CP

Mucic acid lauroyl derivative (**1**) was prepared as previously described (Tian et al 2004). Compound **1** (0.47 g, 0.50 mmol) was mixed with thionyl chloride (20 ml, 270 mmol) and heated to reflux temperature for 4 hours. After cooling to room temperature, the excess thionyl chloride was removed by rotary evaporation. The acyl chloride intermediate was dissolved in 5.0 ml anhydrous methylene chloride solution with 2.0 ml pyridine. Heterobifunctional poly(ethylene glycol) (HCl·NH_2-PEG-COOH) (M_w = 5.0 kDa) (0.50 g, 0.10 mmol) in 5.0 ml methylene chloride solution was added dropwise over 2 min. After 24 hours stirring at room temperature, the reaction mixture was acidified by 0.1 N HCl aqueous solution (10 ml × 2) and washed by brine (10 ml). The organic portion was dried over sodium sulfate, concentrated by rotary evaporator and added into diethyl ether (60 ml) to precipitate the product.

1CM1CP was obtained as white waxy solid. 0.52 g, 86% yield. ^{1}H NMR ($CDCl_3$) (*d*): 5.59 (d, 1H, C*H*), 5.62 (d, 1H, C*H*) 5.21 (m, 1H, C*H*), 5.02 (m, 1H, C*H*), 3.64 (m, ~0.4kH, CH_2 on PEG), 2.38 (t, 4H, CH_2), 2.21 (t, 4H, CH_2), 2.57 (t, 2H, CH_2-COOH of PEG), 1.61 (m, 4H, CH_2), 1.51 (m, 4H, CH_2), 1.25 (m, 48H, CH_2), 0.88 (t, 12H, CH_3). IR (KBr, cm^{-1}): 2911 (C-H), 1754 (C = O), 1250, 1105, (C-O). T_m: 58.0–59.5 °C; GPC: M_w: 5500; PDI: 1.1.

Synthesis of 1BM

Molecule **1** (0.94 g, 1.0 mmol) was mixed with thionyl chloride (20 ml, 270 mmol) and heated to reflux temperature for 4 hours. After cooling to room temperature, the excess thionyl chloride was removed by rotary evaporation. A solution of anhydrous THF (10 ml) and pyridine (5.0 ml) was added to the reaction mixture. 4-Hydroxybenzoic acid (0.55 g, 4.0 mmol) dissolved in THF (5.0 ml) was added dropwise over 2 min at 0 °C. The reaction was warmed to room temperature and stirred for 6 hours. The reaction was quenched by adding 1 N HCl (400 ml) to the reaction mixture. The solid was collected by vacuum filtration and obtained as intermediate product, **2.**

Intermediate **2** was obtained as white solid, 0.89 g, 75% yield. ^{1}H NMR ($CDCl_3$) (*d*): 8.02 (d, 4H, Ar*H*), 6.95 (d, 4H, Ar*H*), 5.59 (m, 2H, C*H*), 4.94 (m, 2H, C*H*), 2.32 (m, 8H, CH_2), 1.49 (m, 8H, CH_2), 1.25 (m, 48H, CH_2), 0.86 (t, 12H, CH_3). IR (KBr, cm^{-1}): 2930 (C-H), 1752 (C = O), 1250, 1148 (C-O), 742 (Aromatic C-C). T_m: 154.5–156.5 °C. FW: 1167; MS: 1165.5.

Intermediate **2** (0.59 g, 0.50 mmol), mPEG (M_w = 5.0 kDa, after azeotropic distillation) (0.50 g, 0.10 mmol) and DPTS (0.16 g, 0.50 mmol) were dissolved in methylene chloride (10 ml) and DMF (1.5 ml) solution. 1 M DCC in methylene chloride solution (1.0 ml, 1.0 mmol) was added slowly. After 24 hours stirring at room temperature, the side product was removed by filtration. The organic solution was washed by 0.1 N HCl aqueous solution (10 ml × 2) and brine (10 ml). The organic portion was dried over sodium sulfate and concentrated by rotary evaporator. Diethyl ether (15 ml) was added to precipitate the product 1BM. Additional ethyl ether (15 ml × 2) was used to wash the product.

1BM was obtained as white waxy solid. 0.54 g, 88% yield. ^{1}H NMR ($CDCl_3$) (*d*): 8.00 (d, 4H, Ar*H*), 6.93 (d, 4H, Ar*H*), 5.60 (m, 2H, C*H*), 4.94 (m, 2H, C*H*), 2.31 (m, 8H, CH_2), 1.47 (m, 8H, CH_2), 1.25 (m, 48H, CH_2), 0.88 (t, 12H, CH_3). IR (KBr, cm^{-1}): 2956 (C-H), 1755 (C = O), 1258, 1106 (C-O), 733 (Aromatic C-C). T_m: 55.4–56.5 °C. GPC: M_w: 5500; PDI: 1.2.

Synthesis of 2CM

Compound 1CM (0.60 g, 0.10 mmol; after azeotropic distillation with toluene) and NHS (0.50 g, 0.43 mmol) were dissolved in 20 ml methylene chloride and DMF (0.8 ml). DCC in methylene chloride (0.50 ml, 0.50 mol) was added dropwise under argon. After 12 h, the side product was removed by vacuum filtration. The isolated solution was directly reacted with β-glutamic acid (0.020 g, 0.43 mmol) in the present of triethylamine (1.0 ml, 7.0 mmol). After 8 hours, the reaction mixture was washed by 0.1 N HCl aqueous solution (10 ml × 2), brine (10 ml), dried over sodium sulfate and concentrated by rotary evaporator. Diethyl ether (15 ml) was added to precipitate the product 2CM.

2CM was obtained as white waxy solid. 0.43 g, 71% yield. ^{1}H NMR ($CDCl_3$) (*d*): 5.62 (m, 2H, C*H*), 5.08 (m, H, C*H*), 3.66 (m, ~0.4kH, CH_2 on PEG), 2.38 (t, 4H, CH_2), 2.21 (t, 4H, CH_2), 1.61 (m, 4H, CH_2), 1.51 (m, 4H, CH_2), 1.25 (m, 48H, CH_2), 0.88 (t, 12H, CH_3). IR (KBr, cm^{-1}): 2925 (C-H), 1750 (C = O), 1229, 1146 (C-O). T_m: 54.6–55.2 °C. GPC: M_w: 5500; PDI: 1.2.

Synthesis of 0BM

Compound 1CM (0.60 g, 0.10 mmol; after azeotropic distillation with toluene), DPTS (0.31 g, 1.0 mmol) and p-phenetidine (0.80 ml, 1.0 mmol) were dissolved in methylene chloride (20 ml). DCC in methylene chloride (0.20 ml, 0.20 mol) was added dropwise under argon. After

12 h, the side product was removed by vacuum filtration. The organic portion was washed by 0.1 N HCl solution (10 ml × 2), brine (10 ml), dried over sodium sulfate and concentrated under rotary evaporator. Diethyl ether (15 ml) was added to precipitate the product.

0BM was obtained as white waxy solid. 0.56 g, 92% yield. ^{1}H NMR ($CDCl_3$) (*d*): 7.21 (d, 2H, Ar*H*), 6.71 (d, 2H, Ar*H*), 5.78 (d, 1H, C*H*), 5.49 (d, 1H, C*H*) 5.38 (m, 1H, C*H*), 4.95 (m, 1H, C*H*), 3.66 (m, ~0.4kH, CH_2 on PEG), 2.38 (t, 4H, CH_2), 2.21 (t, 4H, CH_2), 1.61 (m, 4H, CH_2), 1.51 (m, 4H, CH_2), 1.25 (m, 48H, CH_2), 0.88 (t, 12H, CH_3). IR (KBr, cm^{-1}): 2917 (C-H), 1737 (C = O), 1250, 1120 (C-O), 780 (Aromatic C-C). T_m: 55.5–57.2 °C.GPC: M_w: 5500; PDI: 1.2.

Dynamic light scattering study

Dynamic light scattering (DLS) analyses were performed using a Malvern Instruments Zetasizer Nano ZS-90 instrument (Southboro, MA), with reproducibility being verified by collection and comparison of sequential measurements. Polymer solutions (1.0 wt %) in phosphate buffered aqueous solution (PBS) (pH 7.4) were prepared. Measurements were performed in triplicate at a 90° scattering angle at 25 °C. Z-average sizes and standard deviation of polymers in solution were collected and analyzed.

Fluorescence spectroscopy

Critical micelle concentration (CMC) measurements were carried out on a Spex fluoroMax (Piscataway, NJ) spectrofluorometer at 25 °C. Using pyrene as the probe molecule, a stock solution at 5.00×10^{-7} M in pH 7.4 PBS solution was prepared. Polymer samples were dissolved in the stock pyrene solutions then diluted to specific concentrations. Excitation was performed from 300 nm to 360 nm, using 390 nm as the emission wavelength. Pyrene maximum absorption shifted from 332 nm to 334.5 nm upon secondary micelle formation. The ratio of absorption of polymer (334.5 nm) to pyrene only (332 nm) was plotted as the logarithm of polymer concentrations. The inflection point of the curves was taken as CMC.

Zeta potential

Charge densities of all polymeric micelle solutions were measured by the zeta potential method using a Malvern Instruments Zetasizer Nano ZS-90 instrument (Southboro, MA), with reproducibility verified by collection and comparison of sequential measurements. Instrument settings and calculation parameters were defined as temperature at 25 °C, dispersant viscosity at 0.89 cP and dielectric constant of 78.5. The viscosity of the samples was estimated to be that of water. All the samples measured were prepared at 10^{-4} M in PBS solution (pH 7.4).

Preparation of micelles for in vitro testing

Micelles were freshly prepared and used within 7 days at 10^{-4} M in serum-free RPMI medium (without FBS). The micelles were then combined with serum-free RPMI and/or hoxLDL to create a final macromolecule concentration of 10^{-6} M.

Lipoprotein model: LDL oxidation

Highly oxidized LDL (hoxLDL) was prepared within five days of each experiment. BODIPY-labeled and unlabeled human plasma derived LDL (Molecular Probes, OR) was oxidized for 18 hours in the presence of 10 μM $CuSO_4$ (Sigma) at 37 °C and 5% CO_2 (Oorni et al 1997; Chang et al 2001). The oxidation was stopped with 0.01% w/v EDTA. Thiobarbituric acid reactive substances (TBARS), lipid hydroperoxide (LPO), conjugated dienes, and electrophoretic mobility (with the help of Dr. Schaich) was performed to ensure accurate and consistent oxidation levels were attained.

LDL internalization

The internalization of hoxLDL by macrophage cells was assayed by incubating fluorescently labeled hoxLDL (10ug/mL) with IC21 macrophages for 24 hours at 37 °C and 5% CO_2. The cells were then washed twice with serum-free RPMI medium. The cell-associated fluorescence was measured by acquiring images on a confocal microscope (Sun Microsystems, Santa Clara, CA) and quantifying the fluorescence intensity using Image Pro Plus 5.1 software (Media Cybernetics, San Diego, CA) and normalized to cell number.

Cell culture

IC21 macrophages, a well established differentiated murine cell line acquired from ATCC, were used for all studies. The cells have morphology and structure comparable to that of freshly isolated activated mouse peritoneal macrophages, and have demonstrated LDL receptor activity (Traber et al 1981). IC21 cells degrade acetylated LDL and thus an acceptable model for the study of cholesterol and lipoprotein metabolism by macrophages. These cells are an economical alternative to freshly isolated mouse peritoneal macrophages. The cells were propagated with RPMI media containing 0.4 mM Ca^{2+} and Mg^{2+}, (ATCC) and supplemented with 10% fetal bovine serum (FBS). The cells were maintained in an incubator with 5% CO_2 at

37 °C and harvested prior to reaching confluence. All cell assays were performed in triplicate.

Results

Synthesis of the macromolecules

Several different amphiphilic macromolecules were synthesized in which the number and location of carboxylate groups were modified (Figure 3).

The 1CM, 0CM and 1CP were prepared as described in previous work (Chnari et al 2006). The design rationale for each macromolecule is as follows. 1CM1CP probes the combinatorial activity of a carboxylic acid present in both the hydrophilic and hydrophobic blocks of AScMs. It was successfully synthesized by coupling (NH_2-PEG-COOH) with mucic acid acyl derivatives (1) activated as acyl chloride. 1BM was prepared to investigate any differences between aliphatic and aromatic carboxylates, in this molecule, carboxylates are located in the hydrophobic domain. Our first attempt to generate an aromatic carboxylate group was not successful; we attempted to couple molecule 1CM directly with 4-hydroxybenzoic acid. However, the low nucleophilicity of the phenol yielded unacceptably low coupling efficiencies. Instead, we prepared the symmetric intermediate (2), which was easy to purify and then successfully coupled with mPEG-OH (5k) to obtain 1BM. The macromolecule 0BM was prepared as a control for 1BM and synthesized through direct esterification of the carboxylate on polymer 1CM. 2CM was designed to study how two carboxylates in the hydrophobic block may synergistically influence hoxLDL uptake. Overall, all coupling reactions were achieved in reasonably high coupling efficiency and high yield. All seven macromolecules displayed a comparable molecular weights (~5500) and melting temperatures (~56 °C).

Physical properties of the AScMs

The molecules are similar in size (23–27 nm) in aqueous media (Table 1) except for 2CM, which is slightly larger (~35 nm), and all macromolecules display monomodal size distributions. The CMC values are in similar range, again with the exception of 2CM, which has the

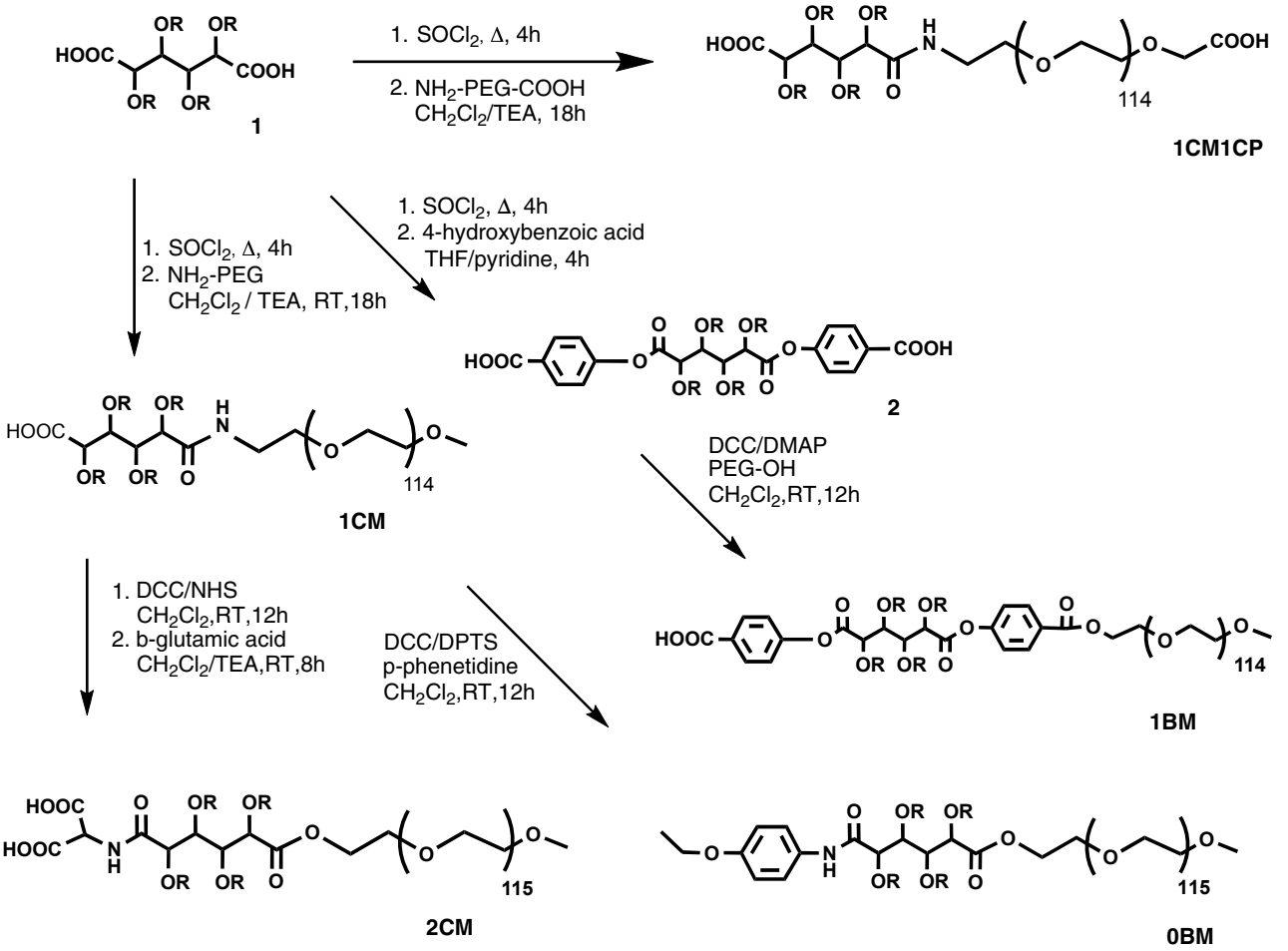

Figure 3 Synthetic outline for the amphiphilic macromolecules.

Table 1 Particle sizes, critical micelle concentrations and zeta-potential values of the amphiphilic macromolecules at pH 7.4

	1CM	0CM	1CP	1CM1CP	1BM	2CM	0BM
Z-average size (nm) at 10^{-4}M	23.2 ± 5.2	27.4 ± 2.5	23.6 ± 5.9	23.1 ± 4.8	23.4 ± 3.7	35.1 ± 4.7	23.9 ± 4.2
CMC (M)	3.2×10^{-7}	5.7×10^{-7}	1.0×10^{-7}	8.8×10^{-7}	7.0×10^{-7}	1.8×10^{-6}	7.8×10^{-7}
Zeta-potential (mV) at 10^{-4}M	−10.4	−0.47	−9.60	−20.1	−15.3	−9.20	−3.46

highest CMC value (1.8×10^{-6} M); the CMC values is approximately 7 times larger than the CMC of 1CM, for example.

With respect to charge density, the polymers 0CM and 0BM are charge neutral yet still register slightly negative zeta potential values (Table 1). 1CM, 1CP and 2CM, display a similar zeta potential value (~ –10mV). Solutions of 1CM1CP display the most negative zeta potential (~ –20 mV), which is double the values for 1CM, 1CP and 2CM.

Highly-oxidized LDL uptake inhibition studies

At 24 hours, hoxLDL uptake in macrophages was significantly reduced in the presence of the anionic nano-sized micelles, namely 1CM, 1CP, 1CM1CP, 2CM and 1BM (Figure 4). The degree of uptake was normalized to controls without polymers present; positive controls included the neutral micelles (0CM and 0BM). Among the effective hoxLDL uptake inhibitors, the 1CM1CP micelles resulted in the highest inhibition of hoxLDL uptake, reducing hoxLDL internalization more significantly ($p < 0.05$) than all the other polymer micelles.

Discussion

Synthesis and solution-based properties

Micelle formation and nanoscale size are both important in hoxLDL inhibition; our hypothesis about the macrophage receptors is that they are slightly positively charged, such that nanoscale micelles with a high density of negative charges are more accessible via electrostatic interactions.

All seven amphiphilic macromolecules self-organized to form micelles in aqueous solutions, as indicated by the CMC values near 10^{-6} to10^{-7} M. The critical micelle concentration (CMC) is a crucial parameter that measures the stability of amphiphiles. All amphiphilic macromolecules have relatively low CMC values (from 10^{-6} to 10^{-7} M), a critical characteristic for biological applications as low CMC values indicate higher stability upon dilution in blood plasma. Most of the AScMs have similar CMC values, indicating that a single negative charge does not prevent self-aggregation into

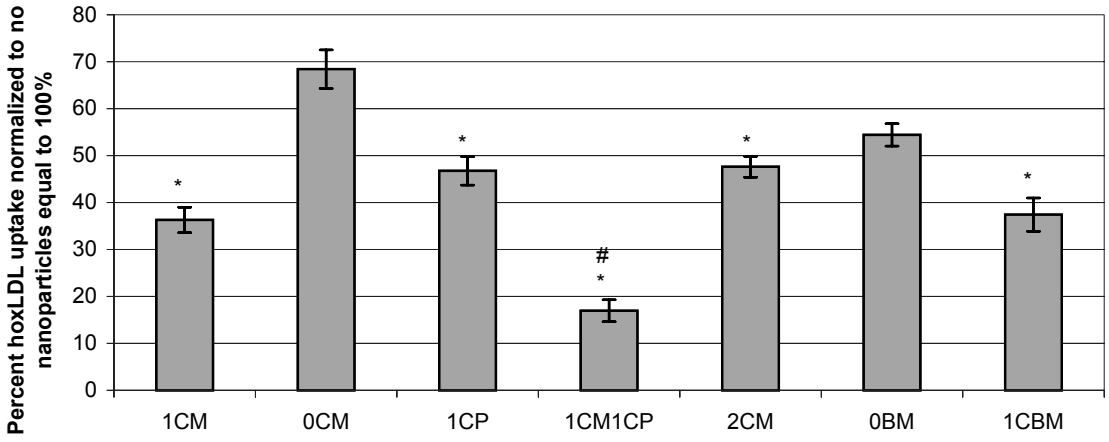

Figure 4 After 24 hours, percent of hoxLDL uptake by macrophages in the presence of amphiphilic macromolecules, compared to hoxLDL alone. Macromolecule concentration is 10^{-6} M.

* represents a significant decrease ($P < 0.05$) in comparison to hoxLDL alone.

represents a significant decrease ($P < 0.05$) in comparison to hoxLDL with 1BM or 1CM.

micelles at pH 7.4. Notably, molecule 2CM has a relatively higher CMC value compared to the other macromolecules. Two aliphatic carboxylate groups on hydrophobic domain of polymeric micelles appear to slightly inhibit micelle formation, possibly due to the repulsion between adjacent negative charges formed in slightly basic (pH 7.4) solution.

Similar to the CMC data, molecule 2CM displays different behavior than the other macromolecules in terms of size. The micellar sizes of all AScMs, except 2CM, are approximately 20 nm (Table 1), indicating that a single negative charge does not change the micelle aggregation size. In contrast, molecule 2CM is larger in size (35 nm) than the other macromolecules. Compared with the other macromolecules, 2CM is relatively less hydrophobic due to the presence of two carboxylates in the hydrophobic block, resulting in a "looser" aggregation or larger size.

Zeta potential measurements determines the surface charge densities, which is expected to be negative for the carboxylate-containing amphiphilic macromolecules. The neutral macromolecules (0CM and 0BM) registered slight negative charges (–3.5 mV and –0.4 mV, respectively). 1BM has a slightly more negative zeta potential than 1CM as benzoic acid is more acidic than the aliphatic carboxylic acid. Notably, 1CM1CP has the most negative value (–20 mV) likely because it contains two carboxylate groups, one in the hydrophobic block and one in the hydrophilic block. Molecule 2CM also bears two negative charges, but both carboxylates reside within the hydrophobic core. As a result, the charge density does not increase in comparison with 1CM.

Inhibition of hoxLDL uptake by amphiphilic nanoparticles

The uncontrollable internalization of hoxLDL by macrophage cells is an essential aspect in atherosclerotic progression (Patel et al 2000). It has previously been proven that 1CM molecules significantly reduce hoxLDL uptake through blockage of SR-A and CD36 scavenger receptors (Chnari et al 2006). The mechanism that leads to enhanced hoxLDL internalization with the anionic micelle particles relative to similar neutral polymers is not completely understood; therefore, nanoparticles with anionic groups placed in precise locations were prepared and evaluated.

The key finding in this study is that charge alone does not determine the extent of hoxLDL internalization reduction by macrophage cells. 1CM1CP is the most effective macromolecule in reducing hoxLDL internalization, while the similarly charged 2CM reduced hoxLDL uptake even less than 1CM. We hypothesize that the size of the 2CM might modulate the behavior of nanoparticle binding to the scavenger receptors. Scavenger receptors typically bind to particles and are then internalized through clathrin-coated pits (Platt and Gordon 2001). Previous studies have shown that the increased size of PEGylated nanoparticles, nanoscale iron oxide contrast agents, and colloids can promote their scavenger receptor mediated uptake in macrophages (Moghimi and Szebeni 2003; Raynal et al 2004; Vonarbourg et al 2006). However, consequences for scavenger receptor ligands such as hoxLDL were not evaluated. The exact mechanism for micellar nanoparticle binding in our system is not clear, but we offer two potential mechanisms. For example, the larger 2CM micellar nanoparticles (~35 nm) may promote the internalization of scavenger receptors in relation to the smaller diameter of 1CM1CP micelle (23.1 nm) and cooperatively facilitate hoxLDL uptake through mechanisms not yet clear. Alternately, the larger nanoparticles may interfere with folding and internalization of scavenger receptors. In either case, the major result is that the reduction in hoxLDL internalization is not addressed from charge alone: The 1CM decreases hoxLDL internalization more significantly than 2CM, even though both exhibit similar values of zeta potential (~ −10 mV).

Conclusion

Several amphiphilic scorpion-like macromolecules were synthesized to investigate how the number and location of carboxylate groups influence hoxLDL inhibition. All macromolecules self-organized into stable nanoscale micelles in an aqueous environment. Carboxylate groups located in the hydrophobic block influenced micelle size and CMC more than carboxylate groups in the hydrophilic block. Overall, molecule 1CM1CP demonstrates several unique characteristics: small size (23.1 nm), low CMC (~10^{-7} M) and high zeta potential (~ –20 mV). The combination of size, nanoparticle stability and charge density appear to be critical for inhibition hoxLDL uptake by macrophages.

Future investigations will focus on identifying the mode of micelle internalization, with a view to support or disprove the hypothesis that micelle diameter affects scavenger receptor occupancy. Mixed micelles will also be tested to determine whether a micelle can be created that will decrease hoxLDL internalization even more significantly than the 1CM1CP alone.

Acknowledgments

The authors gratefully acknowledge funding support from the National Science Foundation (BES-9983272; BES 0201788); and the American Heart Association (9951060T; 0455823T).

We thank Angela Bae and Eric Wydra for assistance in the synthesis and characterization; and Professors Joachim Kohn and Stephan S. Isied (Chemistry, Rutgers) for access to their equipment.

References

Boullier A, Friedman P, Harkewicz R, et al. 2005. Phosphocholine as a pattern recognition ligand for CD36. *J Lipid Res*, 46:969–76.

Brown M , Goldstein J. 1983. Lipoprotein metabolism in the macrophage: implications for cholesterol deposition in atherosclerosis. *Ann Rev Biochem*, 52:223–61.

Broz P, Benito S, Saw C, et al. 2005. Cell targeting by a generic receptor-targeted polymer nanocontainer platform. *J Control Release*, 102:475–88.

Camejo G, Olsson U, Hurt-Camejo E, et al. 2002. The extracellular matrix on atherogenesis and diabetes-associated vascular disease. *Atherosclerosis Supp*, 3–9.

Carella M, Volinia S , Gasparini P. 2003. Nanotechnologies and microchips in genetic diseases. *J Nephrol*, 16:597–602.

Chang M, Potter-Perigo S, Wight T, et al. 2001. Oxidized LDL bind to nonproteoglycan components of smooth muscle extracellular matrices. *J Lipid Res*, 42:824–33.

Chnari E, Nikitczuk J, Uhrich K, et al. 2005. Nanoscale anionic macromolecules can inhibit cellular uptake of differentially oxidized low density lipoproteins. *Biomacromolecules*, 26:3749–58.

Chnari E, Nikitczuk J, Wang J, et al. 2006. Engineered Polymeric nanoparticles for Receptor-Targeted Blockage of Oxidized Low Density Lipoproteins Uptake and Atherogenesis in macrophages. *Biomacromolecules*,

Djordjevic J, Barch M, Uhrich K. 2005. Polymeric micelles based on amphiphilic scorpion-like macromolecules: novel carriers for water-insoluble drugs. *Pharm Res*, 22:24–32.

Endo M, Koyama S, Matsuda Y, et al. 2005. Thrombogenicity and blood coagulation of a microcatheter prepared from carbon nanotube-nylon-based composite. *Nano Lett*, 5:101–5.

Guaderrama-Diaz M, Solis C, Velasco-Loyden G, et al. 2005. Control of scavenger receptor-mediated endocytosis by novel ligands of different length. *Mol Cell Biochem*, 271:123–32.

He W, Ma Z, Yong T, et al. 2005. Fabrication of collagen-coated biodegradable polymer nanofiber mesh and its potential for endothelial cells growth. *Biomaterials*, 26:7606–15.

He W, Yong T, Teo W, et al. 2005. Fabrication and endothelialization of collagen-blended biodegradable polymer nanofibers: potential vascular graft for blood vessel tissue engineering. *Tissue Eng*, 11:1574–88.

Krieger M, Acton S, Ashkenas J, et al. 1993. Molecular Flypaper, Host Defense, and Atherosclerosis: structure, binding properties, and functions of macrophage scavenger receptors. *J Biol Chem*, 268:4569–72.

Ma Z, He W, Yong T, et al. 2005. Grafting of gelatin on electrospun poly(caprolactone) nanofibers to improve endothelial cell spreading and proliferation and to control cell Orientation. *Tissue Eng*, 11:1149–58.

Malinski T. 2005. Understanding nitric oxide physiology in the heart: a nanomedical approach. *Am J Cardiol*, 96:13i–24i.

Meng J, Kong H, Xu H, et al. 2005. Improving the blood compatibility of polyurethane using carbon nanotubes as fillers and its implications to cardiovascular surgery. *J Biomed Mater Res A*, 74:208–14.

Moghimi S, Szebeni J. 2003. Stealth liposomes and long circulating nanoparticles: critical issues in pharmacokinetics, opsonization, and protein-binding properties. *Prog Lipid Res*, 42:463–78.

Olsson U, Ostergren-Lunden G, Moses J. 2001. Glycosaminoglycan-lipoprotein interaction. *Glycoconj J*, 18:789–97.

Oorni K, Pentikainen M, Annila A, et al. 1997. Oxidation of low density lipoprotein particles decreases their ability to bind to human aortic proteoglycans. *J Biol Chem*, 272:21303–11.

Patel R, Moellering D, Murphy-Ullrich J, et al. 2000. Cell signaling by reactive nitrogen and oxygen species in atherosclerosis. *Free Radical Biol Med*, 28:1780–94.

Platt N, Gordon S. 2001. Is the class A macrophage scavenger receptor (SR-A) multifunctional? – The mouse's tale. *J Clin Invest*, 108:649–54.

Raynal I, Prigent P, Peyramaure S, et al. 2004. Macrophage endocytosis of superparamagnetic iron oxide nanoparticles: mechanisms and comparison of ferumoxides and ferumoxtran-10. *Investig Radiology*, 39:56–63.

Steinberg D. 1997. Low density lipoprotein oxidation and its pathobiological significance. *J Biol Chem*, 272:20963–6.

Tao L, Uhrich K. 2006. Novel amphiphilic macromolecules and their in vitro characterization as stabilized micellar drug delivery systems. *J Colloid Interf Sci*, 298:102–10.

Thom T, Haase N, Rosamond W, et al. 2006. Heart Disease and Stroke Statistics – 2006 Update: A Report From the American Heart Association Statistics Committee and Stroke Statistics Subcommittee. *Circulation*, 113:e85–e151.

Tian L, Yam L, Zhou N, et al. 2004. Amphiphilic scorpion-like macromolecules: design, synthesis, and characterization. *Macromolecules*, 37:538–42.

Traber M, Defendi V, Kayden H. 1981. Receptor activities for low-density lipoprotein and acetylated low-density lipoprotein in a mouse macrophage cell line (IC21) and in human monocyte-derived macrophages. *J Exp Med*, 154:1852–67.

Vonarbourg A, Passirani C, Saulnier P, et al. 2006. Evaluation of pegylated lipid nanocapsules versus complement system activation and macrophage uptake. *J Biomed Mater Res*, 78A:620–8.

Williams K , Tabas I. 1995. The response-to-retention hypothesis of early atherogenesis. *Arterioscler Thromb Vasc Biol*, 15:551–61.

Yoshiizumi K, Nakajima F, Dobashi R, et al. 2004. 2,4-Bis(octadecanoyl amino)benzenesulfonic acid sodium salt as a novel scavenger receptor inhibitor with low molecular weight. *Bioorg Med Chem Lett*, 14:2791–5.